



## Article

# Impact of Elevated Levels of Dissolved CO<sub>2</sub> on Performance and Proteome Response of an Industrial 2'-Fucosyllactose Producing *Escherichia coli* Strain

Greta Gecse<sup>1,2</sup>, André Vente<sup>3</sup> , Mogens Kilstруп<sup>2</sup> , Peter Becker<sup>1</sup> and Ted Johanson<sup>1,\*</sup>

<sup>1</sup> HMO Innovation and Business Development, Royal DSM, Kogle Allé 4, 2970 Hørsholm, Denmark; greta.gecse@dsm.com (G.G.); p.becker@dsm.com (P.B.)

<sup>2</sup> Department of Biotechnology and Biomedicine, Technical University of Denmark, Sølltofts Plads Building 221, 2800 Kgs. Lyngby, Denmark; mki@bio.dtu.dk

<sup>3</sup> Center for Analytical Innovation, Biodata & Translation, Science & Innovation, Royal DSM, Alexander Fleminglaan 1, 2613 AX Delft, The Netherlands; andre.vente@dsm.com

\* Correspondence: ted.johanson@dsm.com

**Abstract:** Large-scale microbial industrial fermentations have significantly higher absolute pressure and dissolved CO<sub>2</sub> concentrations than otherwise comparable laboratory-scale processes. Yet the effect of increased dissolved CO<sub>2</sub> (dCO<sub>2</sub>) levels is rarely addressed in the literature. In the current work, we have investigated the impact of industrial levels of dCO<sub>2</sub> (measured as the partial pressure of CO<sub>2</sub>, pCO<sub>2</sub>) in an *Escherichia coli*-based fed-batch process producing the human milk oligosaccharide 2'-fucosyllactose (2'-FL). The study evaluated the effect of high pCO<sub>2</sub> levels in both carbon-limited (C-limited) and carbon/nitrogen-limited (C/N-limited) fed-batch processes. High-cell density cultures were sparged with 10%, 15%, 20%, or 30% CO<sub>2</sub> in the inlet air to cover and exceed the levels observed in the industrial scale process. While the 10% enrichment was estimated to achieve similar or higher pCO<sub>2</sub> levels as the large-scale fermentation it did not impact the performance of the process. The product and biomass yields started being affected above 15% CO<sub>2</sub> enrichment, while 30% impaired the cultures completely. Quantitative proteomics analysis of the C-limited process showed that 15% CO<sub>2</sub> enrichment affected the culture on the protein level, but to a much smaller degree than expected. A more significant impact was seen in the dual C/N limited process, which likely stemmed from the effect pCO<sub>2</sub> had on nitrogen availability. The results demonstrated that microbial cultures can be seriously affected by elevated CO<sub>2</sub> levels, albeit at higher levels than expected.

**Keywords:** scale-down; fermentation; physiology; *Escherichia coli*; proteome; dissolved carbon dioxide; 2'-fucosyllactose; HMO; large-scale fermentation



**Citation:** Gecse, G.; Vente, A.; Kilstруп, M.; Becker, P.; Johanson, T. Impact of Elevated Levels of Dissolved CO<sub>2</sub> on Performance and Proteome Response of an Industrial 2'-Fucosyllactose Producing *Escherichia coli* Strain. *Microorganisms* **2022**, *10*, 1145. <https://doi.org/10.3390/microorganisms10061145>

Academic Editors: Peter Neubauer and Christoph Herwig

Received: 19 April 2022

Accepted: 24 May 2022

Published: 1 June 2022

**Publisher's Note:** MDPI stays neutral with regard to jurisdictional claims in published maps and institutional affiliations.



**Copyright:** © 2022 by the authors. Licensee MDPI, Basel, Switzerland. This article is an open access article distributed under the terms and conditions of the Creative Commons Attribution (CC BY) license (<https://creativecommons.org/licenses/by/4.0/>).

## 1. Introduction

Human milk oligosaccharides (HMOs) constitute important and highly abundant components of mother's milk that provide many health benefits to the neonate including the growth of beneficial gut bacteria and the improved function of the intestinal barrier [1–3]. Out of the HMOs in mother's milk, 2'-fucosyllactose (2'-FL) is the most abundant [4] and therefore the most interesting from a commercial point of view. Today, 2'-FL is almost exclusively produced by fermentation where it is formed in vivo by the decoration of lactose with fucose through the action of a heterologous fucosyl transferase (Figure 1). *E. coli* has been the organism of choice for 2'-FL biosynthesis from the very beginning. In addition to being a well-known and easily modifiable workhorse in industrial biotechnology, it has the advantages of having a native lactose uptake system and a native colanic acid pathway to produce the activated GDP-L-fucose required for the fucosyl transferase reaction. Using *E. coli* as production host fermentations with 2'-FL titers of up to 180 g/L has been reported [5].



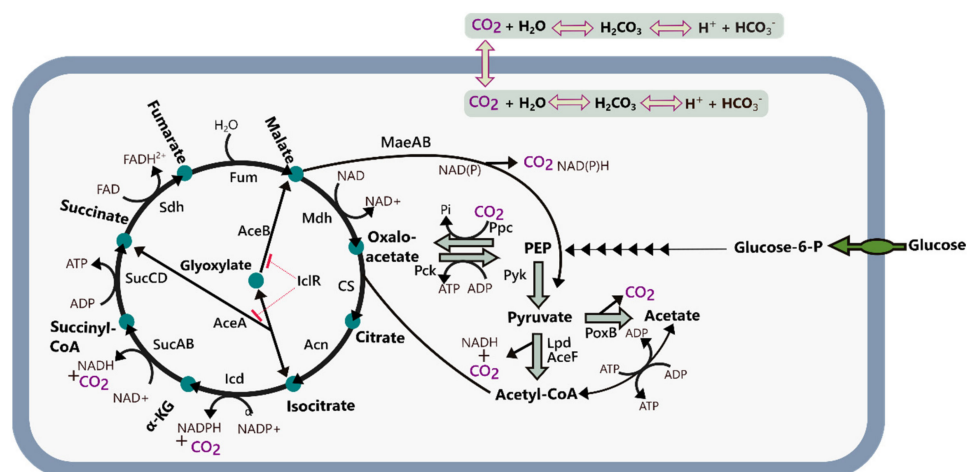


**Figure 2.** Schematic overview of the central carbon metabolism of *E. coli* including the CO<sub>2</sub> producing/consuming reactions. Abbreviations: α-KG: α-ketoglutarate; Icd: isocitrate dehydrogenase; Acn: aconitate hydratase; GltA: citrate synthase; IclR: isocitrate lyase repressor; Mdh: malate-dehydrogenase; Fum: fumarase; Sdh: succinate:quinone oxidoreductase; SucCD: succinyl-CoA synthetase; SucAB: 2-oxoglutarate decarboxylase; PEP: phosphoenolpyruvate; Pyk: pyruvate kinase; Lpd: lipoamide dehydrogenase; AceF: pyruvate dehydrogenase; PoxB: pyruvate oxidase; Ppc: phosphoenolpyruvate carboxylase; Pck: phosphoenolpyruvate carboxykinase; MaeAB: malate dehydrogenase (oxaloacetate-decarboxylating).

Since very little has been published on the impacts of pCO<sub>2</sub> in fed-batch processes, the effects on the performance, physiology, and the proteome resulting from an extended exposure to the pCO<sub>2</sub> levels typically encountered in industry are so far largely unknown or kept secret.

With this study we aimed to characterize the impact of elevated pCO<sub>2</sub> on an *E. coli* based industrial fermentation process. Product yields were determined at different CO<sub>2</sub> enrichment levels and compared to the performance in large-scale operations. The global proteome levels of the laboratory-scale runs were then studied under selected conditions. In addition, as the industrial process was limited on both carbon and nitrogen, the impact of enriched pCO<sub>2</sub> on a C/N-limited process was evaluated and compared to a C-limited process to isolate the impact of CO<sub>2</sub> from any potential differences in nitrogen limitation. To the best of our knowledge, this work shows the impacts of pCO<sub>2</sub> on process performance and bacterial physiology in a high yielding industrial fed-batch process for the first time.

## 2. Materials and Methods

### 2.1. Strain

The strain used in all experiments was derived from *E. coli* K12 DH1 with the genotype: *F*<sup>-</sup>, *L*<sup>-</sup>, *gyrA96*, *recA1*, *relA1*, *endA1*, *thi-1*, *hsdR17*, *supE44*. Additional modifications were made to generate the Strain 0: (i) deletion of *lacZ* to abolish β-galactosidase activity and prevent hydrolysis of lactose to glucose and galactose; (ii) deletion of the galactoside O-acetyltransferase gene *lacA*, which encodes for an enzyme that acetylates the galactose residues of oligosaccharides and would thereby lead to increased carbohydrate-type impurities; (iii) deletion of the *wcaJ* gene that encodes a lipid carrier transferase involved in colanic acid biosynthesis (colanic acid is an extracellular polysaccharide containing fucose and its overproduction dramatically increases the viscosity of the culture medium and acts as a drain on GDP-L-Fucose); (iv) deletion of the glucan biosynthesis glucosyltransferase H gene *mdoH* (the MdoH enzyme is involved in the biosynthesis of periplasmic glucans, the presence of which complicates the isolation and purification of targeted oligosaccharides); (v) deletion of the transcriptional repressor *glpR* to achieve higher expression levels of the genes controlled by the modified P<sub>glpF</sub> promoter used for 2'-FL synthesis; (vi) deletion of the lactose repressor *lacI* to remove the need for addition of isopropyl

$\beta$ -D-1-thiogalactopyranoside to induce expression of the Plac promoter controlled lactose permease encoded by *lacY*. Strain 0 was further engineered to generate the 2'-FL producing strain (Figure 1) used for the experiments by chromosomally integrating two copies of the alpha-1,2-fucosyltransferase *futC* from *Helicobacter pylori* 26,695 (homologous to NCBI Accession nr. WP\_080473865.1 with two additional amino acids (LG) at the C-terminus) under the control of a modified PglpF promoter [29], and an additional copy of the colanic acid operon (*gmd-wcaG-wcaH-wcaI-manC-manB*) under the control of the same modified PglpF promoter. The modified PglpF promoter and the Plac promoter, sans *lacI*, were both automatically induced in the absence of catabolite repression. Thus, high level expression of the colanic acid genes, *futC* and *lacY*, were initiated when the cultures transitioned from catabolically repressed exponential growth in the batch phase into glucose limited growth in the fed-batch phase. Cryovials containing the strain in 25% (*v/v*) glycerol solution were stored at  $-80\text{ }^{\circ}\text{C}$  prior to use.

## 2.2. Precultures

Precultures were prepared in two steps and were cultivated overnight at  $33\text{ }^{\circ}\text{C}$  with 200 rpm shaking. The frozen *E. coli* stock was used to inoculate a preculture with 10 mL minimal glucose media in a 50 mL Falcon tube. The medium was composed of 10 g/L  $\text{NH}_4\text{H}_2\text{PO}_4$ , 5 g/L  $\text{KH}_2\text{PO}_4$ , 1 g/L citric acid, 2.35 g/L NaOH, 1.65 g/L KOH, 5 g/L  $\text{K}_2\text{SO}_4$ , 10 g/L trace metal solution, and finally 1 g/L  $\text{MgSO}_4 \cdot 7\text{H}_2\text{O}$  and thiamine solutions, which were sterilized and added separately. A second preculture in a 250 mL baffled shake flask with 50 mL of the same minimal glucose medium was inoculated with the overnight culture to a final optical density at 600 nm ( $\text{OD}_{600}$ ) of 0.25. The shake flask was then incubated at  $33\text{ }^{\circ}\text{C}$  and 200 rpm for 6–9 h until a final  $\text{OD}_{600}$  of 3–5 and thereafter used to inoculate the main culture.

## 2.3. Fed-Batch Bioreactor Cultivations

Lab-scale fermentations were carried out in 2 L Sartorius Biostat B fermenters equipped with an MFCS-monitoring system (Sartorius). The fermentations were glucose limited fed-batch processes using the same minimal medium composition and feed profile as the large-scale process (confidential) with a starting mass of 1.2 kg. Main cultures were inoculated with liquid precultures to a 2% (*v/v*) final ratio. Both the fermentation media and the feed contained glucose and lactose. The DO was controlled by a stirring (700–2000 rpm) and airflow (1–3 VVM) cascade set to 23%. The pH level was kept at 6.8 by  $\text{NH}_4\text{OH}$  titration. The system was equipped with  $\text{pO}_2$  (Hamilton),  $\text{pCO}_2$  (only for a few experiments, iSense 5000i, Mettler and Toledo, Columbus, OH, USA), temperature, and pH (Hamilton) sensors. Statistical analysis of fermentation data was performed in SAS JMP.

## 2.4. $\text{CO}_2$ Enrichment

In the  $\text{CO}_2$  enriched fermentations, pure  $\text{CO}_2$  was added to the airflow inlet and was initiated when the fed-batch phase started. The  $\text{CO}_2$  concentration in the inlet air was kept constant by an airflow controller. The  $\text{pCO}_2$  levels were either monitored with a probe or estimated by superimposing the  $\text{pCO}_2$  in the inlet gas stream with the  $\text{pCO}_2$  levels that were measured in the reference fermentations without enrichment. An overview of all the fermentations performed in this study is presented in Table A1 in the Appendix A.

## 2.5. Calibration of $\text{CO}_2$ Probe

As a proof of concept, the level of  $\text{pCO}_2$  was monitored with a probe (i5000 Mettler and Toledo). The probe was autoclaved in a separate vessel with a batch phase fermentation mineral medium, as described above. After sterilization, the pH was adjusted to 6.8 by  $\text{NH}_4\text{OH}$ , the temperature was set to  $33\text{ }^{\circ}\text{C}$ , and the stirring was set to 700 rpm. A two-point calibration was performed by measuring the  $\text{pCO}_2$  level after sparging media with gas mixtures of 20/80%  $\text{CO}_2/\text{N}_2$  and 8/10/82%  $\text{CO}_2/\text{O}_2/\text{N}_2$ . The calibration process was monitored using i5000 software and saturation was assumed when the values became

stable. The probe was then moved to the fermenter used for the experiments inside a sterile laminar flow bench to avoid contamination. In the industrial scale fermenter, the same process calibration was performed before the probe was mounted in the fermenter prior to sterilization.

### 2.6. Sampling and Analytical Procedures

The 2'-FL, DFL, and lactose levels in the fermentation broth samples were quantified by HPLC. Samples taken from the vessel were immediately diluted with deionized water and boiled for 20 min. After the heat-treatment, the samples were centrifuged for 3 min at  $17,000\times g$  and the resulting supernatant analyzed by HPLC (Dionex Ultimate 3000 RS, Thermo Scientific, Waltham, MA, USA) using a Supelco TSK gel Amide-80 HPLC column with a 68% acetonitril isocratic solvent. The biomass was monitored as bio wet mass (BWM), defined as the weight ratio of the pellet to the pellet and the supernatant after 3 min centrifugation at  $17,000\times g$ . The BWM values were converted into dry cell weight (CDW) using a ratio that was determined in previous experiments (data not shown). Samples for acetate measurements were taken by a 3 mL syringe (HENKE-JECT<sup>®</sup>, Henke, Sass, Wolf GmbH, Tuttlingen, Germany) and were directly filtered through a 0.45  $\mu\text{m}$  cellulose syringe filter (30 mm diameter, Thermo Fisher, Waltham, MA, USA).  $\text{NH}_4^+$  and phosphate levels were estimated from supernatant samples by using Quantofix<sup>®</sup>.

### 2.7. Proteomics Analysis

Cells were harvested at different time points after feed start in the fed-batch process (6, 30, 80, 120 h). The precise timepoints of each condition are listed in Appendix A, Table A1. Fermentation broth was sampled directly into a syringe filled with ice cold 0.9% NaCl solution which diluted the broth approximately 3-fold. The syringe was measured before and after adding the fermentation broth to calculate the dilution factor and the cell weight. The solution was kept on dry ice until transport to the centrifuge. The solution was centrifuged at  $4100\times g$  for 10 min at  $4^\circ\text{C}$ . The pellet was then washed in ice-cold 0.9% NaCl solution and pelleted again by centrifugation for 5 min at  $6000\times g$  at  $4^\circ\text{C}$ . The pellet was then immediately placed on dry ice and transferred into a  $-80^\circ\text{C}$  freezer where it was stored until the analysis.

Proteome analysis was performed at the DSM Biotechnology Center in Delft, NL. Lysis buffer (PreOmics) was added to the frozen cell pellets and the solutions heated for 15 min at  $95^\circ\text{C}$ . For proteomics analysis, lysates were normalized to an equivalent of 10 mg lysed cells followed by reduction, alkylation, and digestion using trypsin. Samples were analyzed in technical triplicates by liquid chromatography tandem mass spectrometry (LC-MS/MS) using a Vanquish UHPLC coupled to a Q Exactive Plus Orbitrap MS (Thermo Fisher Scientific). Peptides were separated via reverse-phase chromatography using a gradient of water with 0.1% formic acid (solvent A) and 80% acetonitrile with 0.1% formic acid (solvent B) from 5% B to 40% B in 20 min with a flow rate of 400  $\mu\text{L}/\text{min}$ . Data-independent acquisition (DIA) was performed with a resolution setting at 17,500 within the 400- to 1200- $m/z$  range and a maximum injection time of 20 ms, followed by 8 high-energy collision-induced dissociation activated (HCD) MS/MS scans with a resolution setting at 17,500 covering the mass range from 400 to 875  $m/z$  using 60Da collision windows.

Data was analyzed with Spectronaut version 14.10 (Biognosys, Schlieren, Switzerland) [30], using the direct DIA approach with a protein database for the specific strain used in the study allowing Trypsin/P specific peptides including 2 missed cleavages, an oxidation on methionine, carbamidomethylated cysteines, and deamidated asparagine and glutamine. Label-free quantification was performed using the top three unique peptides measured for each protein. Retention time alignment was performed on the most abundant signals obtained from peptides measured in all samples, and results were filtered by FDR of 1% followed by normalization of the result using the median ion intensities measured for each sample.

## 2.8. Data Analysis

Proteomics data analysis and differential expression analysis (DEA) were performed in R, using a custom-made package based on limma in R. The protein counts were centralized, and DEA was used to compare the protein expressions at given time points between control and CO<sub>2</sub> enriched conditions. Three different time points were compared from the C-limited fermentations: 6, 30, and 120 h after feed start and two in the C/N-limited fermentations 30 and 120 h after feed start.

The DEA analysis was performed in R using the limma package with linear models. To determine the differentially expressed proteins, standard filtering conditions based on fold change (FC) and significance were used with the following settings: FC > 1.5,  $p < 0.05$ .

## 3. Results

### 3.1. pCO<sub>2</sub> Levels in Industrial and Laboratory Scale

The pCO<sub>2</sub> levels of an industrial 2'-FL process performed in a 450 m<sup>3</sup> fermentation vessel were measured by a commercial probe located close to the bottom of the vessel and compared to a corresponding laboratory process. As expected, the measured pCO<sub>2</sub> levels were significantly higher in the large fermenter with a two–three-fold increase and a peak level of 150–160 mbar (Figure 3). These levels were in a range where previous studies had reported negative effects on *E. coli* cultures, albeit in a batch growth [19]. Follow-up runs using scale-down models with 15% and 30% CO<sub>2</sub> enrichment in the inlet sparging gas were also measured with the CO<sub>2</sub> probe. In addition, scale-down runs with 10% and 20% enrichment were carried out without a probe but had their pCO<sub>2</sub> levels estimated. The measured and estimated pCO<sub>2</sub> levels can be seen in Figure 3.

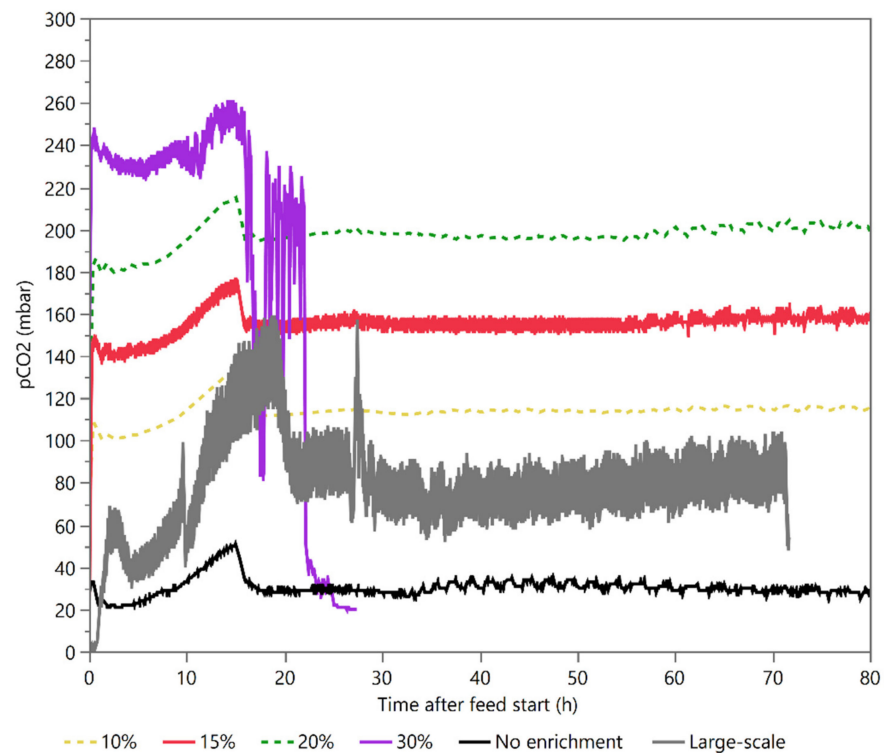


**Figure 3.** Measured and estimated pCO<sub>2</sub> concentrations. pCO<sub>2</sub> concentrations were measured from fermentations with 15% CO<sub>2</sub> enrichment (red), 30% CO<sub>2</sub> enrichment (purple), non-enriched control fermentations (black), and a large-scale fermentation (grey). pCO<sub>2</sub> values from 10% (yellow dashed line) and 20% (green dashed line) enrichments were not measured but estimated from the measurements from the 15% and the control fermentations. The estimated pCO<sub>2</sub> curves are shown as 20 min moving averages of measured pCO<sub>2</sub> data with superimposed values from the inlet air stream to reflect the actual enrichment.

### 3.2. Dual Limitation in the Fermentation Process

The fermentation process in this study had an unusual trait. While initially being C-limited, the process naturally became N-limited approximately 30 h into the fed-batch phase, whereafter it settled into an oscillatory state seemingly shifting back and forth between N-limitation coupled with a slight overflow metabolism and pure C-limitation. This behavior was observed in both large- and laboratory-scale processes and its onset could be observed by following the  $[\text{NH}_4^+]$ , but also by the emergence of obvious oscillations of the on-line parameters such as the pH,  $\text{CO}_2$  evolution, and dissolved oxygen levels (see example in Figure 4A).

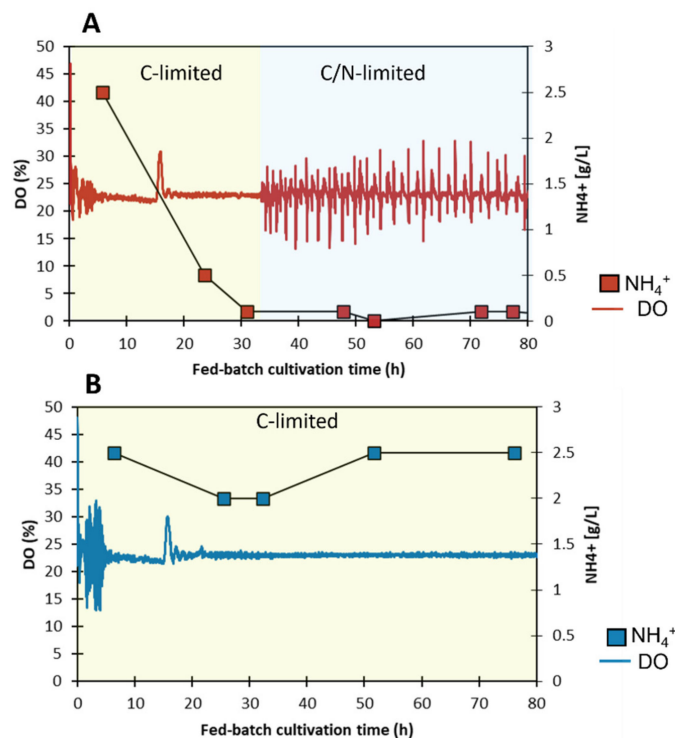


**Figure 4.** Baseline laboratory-scale fed-batch processes without  $\text{CO}_2$  enrichment. (A) C/N-limited process. N-limitation began approximately 30 h after the feed started manifesting as low extracellular  $\text{NH}_4^+$  concentrations and metabolic oscillations in DO, pH,  $\text{CO}_2$ , and other parameters. DO levels are presented as an example. The C-limited phase is marked with yellow and the dual C/N-limited phase with light blue. (B) Sole C-limitation was achieved by supplementation with ammonium sulfate.  $\text{NH}_4^+$  concentrations are shown with square markers.

As N-limitation and C-limitation have very different regulations of gene expression, [31] any change to the degree of N-limitation was expected to have a profound impact on the physiology of the *E. coli* strain. This could include shifts in maintenance requirements, metabolic pathway regulation, and the transcriptome and proteome profiles, which in turn could lead to shifts in biomass and product yields. Since the  $\text{pCO}_2$  level affects pH and thereby indirectly the N-level via the pH titrant  $\text{NH}_4\text{OH}$ , it could potentially reduce or even relieve the impact of N-limitation and thereby obscure other effects caused by increased  $\text{pCO}_2$ . To introduce a control for this potential bias, laboratory cultivations with and without  $\text{pCO}_2$  enrichment with excess nitrogen were also included in the study. In these fermentations, additional  $\text{NH}_4^+$  was supplemented via the base titrant in the form of  $(\text{NH}_4)_2\text{SO}_4$  to keep the  $[\text{NH}_4^+]$  between 2–3 g/L in the fermenter (Figure 4). Having extra nitrogen available for growth also led to a higher biomass (Figure 5) after 50 h of the fed-batch phase. A carbon allocation comparison showed that the carbon from this extra biomass was predominantly taken from the product formation, whereas the  $\text{CO}_2$  evolution was similar (Figure 5). While the allocation to product formation at a large-scale

was initially similar to either C- or C/N-limited laboratory-scale fermentations, it became significantly lower and had a slightly lower biomass after the onset of C/N-limitation. Instead, CO<sub>2</sub> evolution was much higher.

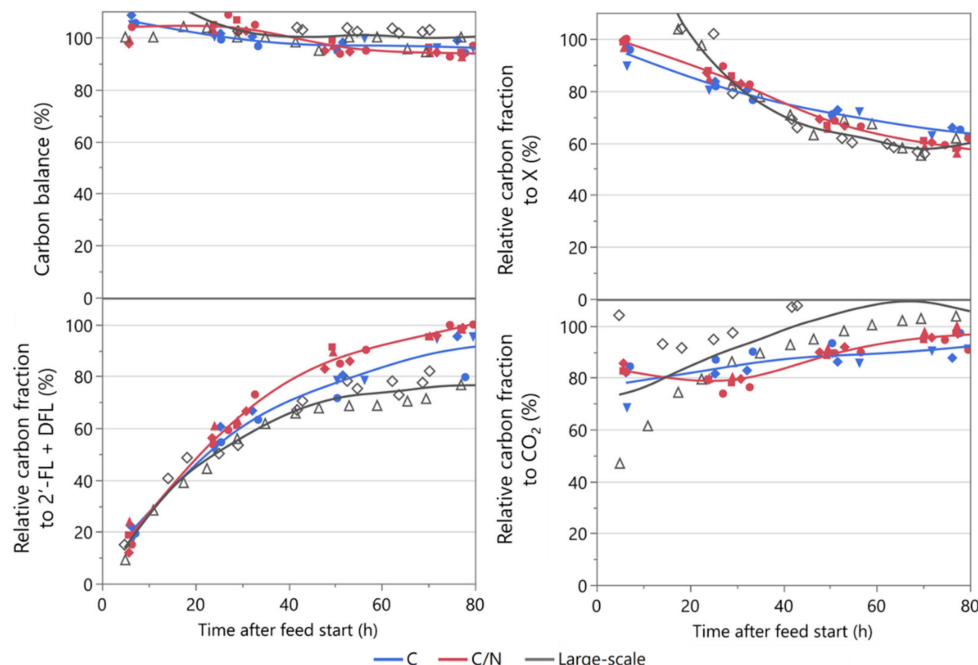


**Figure 5.** Carbon balance and carbon allocation of laboratory and industrial fermentations. Carbon allocation to the products 2'-FL and DFL as well as biomass (X) and CO<sub>2</sub> were estimated from offline and online measurements. Each curve represents three independent experiments from laboratory-scale and two from large-scale processes. The values were relativized by normalizing to the end-point value of the average of the three fermentations without CO<sub>2</sub> enrichment under C/N limitation.

### 3.3. Fermentation Performance with and without pCO<sub>2</sub> Enrichment

To investigate the impact of high pCO<sub>2</sub> levels, both C- and C/N-limited fermentations were compared at different levels of CO<sub>2</sub> enrichment in at least two independent fermentations. Product yields were evaluated as the sum of the carbon allocated to the produced HMOs (2'-FL + DFL) per glucose added. The summary of the 15 fermentations performed during this study is presented in Table 1.

**Table 1.** Relative accumulated biomass and product yield on glucose.

CO <sub>2</sub> Enrichment	Limitation	Number of Replicates	Relative Accumulated Biomass Yield (Y <sub>xs</sub> , %) *	Relative Accumulated Product Yield (Y <sub>ps</sub> , %) *
0	C/N	3	100 ± 6.7	100 ± 8.3
10%	C/N	1	105	104
15%	C/N	3	106 ± 7	96 ± 2.0
20%	C/N	2	128–141	88–90
30%	C/N	2	n/a **	n/a **
0%	C	3	118 ± 5.1	85 ± 9.5
15%	C	2	115–116	89–92
<b>Large-scale</b>	<b>C/N</b>	<b>3</b>	<b>109 ± 4.7</b>	<b>77 ± 2.7</b>

\* Summary of the results shown are either ranges from duplicate fermentations or average values calculated from triplicate fermentations with standard deviations. The values were relativized by normalizing to the average of the end-point value of the three fermentations without CO<sub>2</sub> enrichment under C/N limitation. Y<sub>ps</sub> includes 2'-FL and DFL. \*\* n/a: no stable run achieved under these conditions.

The fermentation that had the closest pCO<sub>2</sub> level to large-scale fermentations was the 10% CO<sub>2</sub> enrichment, which was approximately similar or higher in pCO<sub>2</sub>. (Figure 3).

However, this enrichment did not lead to any observable difference in the performance as measured in the product and biomass yields (Table 1, Figure 6C,D). Increasing the enrichment to 15% pCO<sub>2</sub> led to a slightly increased biomass yield for the C/N limited process and increasing the enrichment further to 20% pCO<sub>2</sub> led to an additional biomass increase (Table 1, Figure 6C,D). The pCO<sub>2</sub> enrichment first had an impact on biomass after 40 h, which corresponded with the onset of N-limitation. In addition to biomass, product yields were also affected at 15% and 20% pCO<sub>2</sub>. Again, this effect started at the onset of N-limitation. A further increase of pCO<sub>2</sub> to 30% caused a marked increase in the base consumption right from the onset of the enrichment and led to a complete loss of culture viability approximately 20 h later (Figure 6C,D). A sample taken at 25 h of fermentation revealed 32.5 g/L acetic acid and 3.7 g/L glutamic acid, showing that the much larger base pull (Appendix C, Figure A1) was caused by acid accumulation.

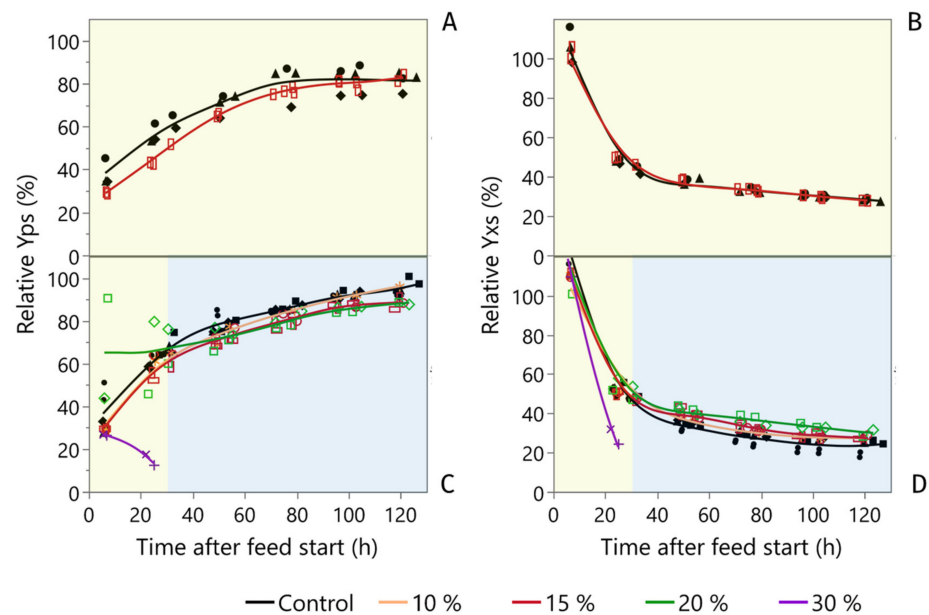


**Figure 6.** Relative product and biomass yields on glucose. (A) Product yield (Yps-2'-FL + DFL) and (B) biomass yield (Yxs), under C-limitation, (C) product yield and (D) biomass yield under C/N-limitation with different levels of CO<sub>2</sub> enrichment. Different marker types represent distinct replicate fermentations. The values were relativized by normalizing to the end-point value of the average of the three fermentations without CO<sub>2</sub> enrichment under C/N limitation.

The 15% pCO<sub>2</sub> enrichment was selected as the focus for the proteomics study and the C- vs. C/N comparison even though it had a higher average pCO<sub>2</sub> level than what was measured in the large-scale fermentation (Figure 3). This decision was taken since it was the lowest pCO<sub>2</sub> level that had a discernible impact on the fermentation. It was therefore considered to have a higher likelihood of undergoing a physiological change that could be resolved in the proteomics data and was still at a level with industrial relevance. In the C-limited study, no impact on biomass yield could be seen with the 15% pCO<sub>2</sub> enrichment (Figure 6B). The enrichment initially led to a lower product yield, but this difference diminished and eventually disappeared over time (Figure 6A). It should be noted that the deviation was high between the three replicates in the control group caused by a potential outlier (Figure 6A, black full diamonds). C-limitation on its own decreased the product yield compared to the regular C/N-limited process with and without CO<sub>2</sub> enrichment. (Table 1).

### 3.4. Proteome Analysis

A timeseries proteomics study was conducted to evaluate the effect of pCO<sub>2</sub> enrichment under C- and C/N limited conditions. The samples from the enriched processes were

compared to their respective 0% references to gain an overview of the impact of elevated pCO<sub>2</sub> levels on the bacterial physiology. For the 15% pCO<sub>2</sub> enrichment analysis, cells were harvested from three or four time points in at least duplicate fermentations. The 10% and 20% pCO<sub>2</sub> enriched fermentation data was derived from single experiments; however, the data in general were very reproducible and therefore single determinations were still included in the data analysis. In the study, which was not optimized for membrane proteins, a total of 1546 proteins were detected.

### 3.4.1. Identification of Differentially Expressed Proteins

The number of significantly differentially expressed (DE) proteins between 0% and 15% CO<sub>2</sub> enriched conditions at given timepoints are presented in Table 2. In general, there were higher numbers of differentially expressed proteins in the C/N limited condition. A functional Gene Ontology (GO) enrichment analysis was performed to find patterns and used to divide these differentially expressed proteins into groups (Figure 7). GO enrichment analysis revealed that the identified functional groups from the middle and late fermentation phases were similar. The highest-ranking groups were related to nitrogen and carbon metabolism and transportation. In the middle-fermentation phase, tricarboxylic acid (TCA) cycle and arginine biosynthesis related proteins were upregulated with CO<sub>2</sub> enrichment, while transport and glutamate related proteins were downregulated. At the late fermentation stage, transport (especially ABC transporters) and glutamate related proteins were downregulated, whereas glycolysis and pyruvate metabolism related proteins were upregulated (Figure 7).

**Table 2.** Summary of differentially expressed proteins at various timepoints. Upregulation means higher expression in the CO<sub>2</sub> enriched condition. Significant differential expression was defined as  $p < 0.05$  and  $FC > 1.5$ .

C-Limited			C/N-Limited		
Comparison	Fermentation Phase	Number of DE Proteins	Comparison	Fermentation Phase	Number of DE Proteins
Control vs. 15% enriched	Early	22 (9↑,13↓)	Control vs. 15% enriched	Early	N/A
	Mid	17 (9↑,8↓)		Mid	139 (98↑,41↓)
	End	5 (3↑,2↓)		End	218 (163↑,55↓)

After the number of differentially expressed (DE) proteins, the number is specified into numbers of upregulated and downregulated (followed by ↑ and ↓, respectively)

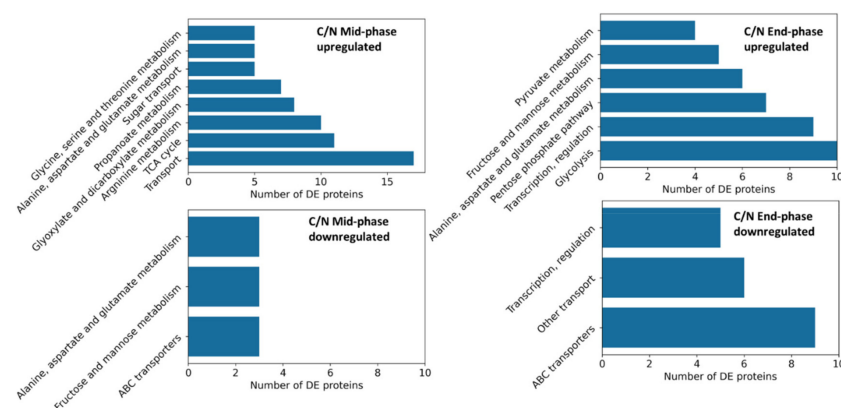


**Figure 7.** GO enrichment of differentially expressed proteins of 15% versus 0% pCO<sub>2</sub> enriched cultures under C/N-limited conditions.

Fewer differentially expressed proteins were identified in the C-limited condition (Table 2). It was therefore not feasible to quantitatively group the differentially expressed proteins based on their functions. In the mid-fermentation phase, many of the upregulated proteins were related to acid stress response, such as GadA, GlsA, and GadB. In the late fermentation phase, there were only five differentially expressed proteins left. Three pro-

teins were upregulated with CO<sub>2</sub> enrichment: Ada (3-fold), DmlA (1.7 fold), and EutM (1.5-fold); two were downregulated FlgM (2.5 fold) and DadA, (4 fold). Interestingly, flagellin synthesis-related proteins were downregulated in all timepoints. On the other hand, CsgD, curli operon transcriptional regulatory protein, LolB, outer membrane lipoprotein, and PspC phage shock proteins were all upregulated. These could potentially serve as a protection from the increased pCO<sub>2</sub>.

There were only a few identified proteins that were commonly changed for the C- and C/N-samples as a result of pCO<sub>2</sub> enrichment. These proteins were: GlsA, DmlA, GltA and Mdh. Thus, malate dehydrogenase and glutamine/glutamate metabolisms were affected by the increased CO<sub>2</sub> levels regardless of the nitrogen limitation.

### 3.4.2. Time Course Expression Changes of 2'-FL Production and TCA Related Proteins

To investigate the underlying cause of the lower product yields in the enriched fermentations, the expression profiles of proteins involved in the 2'-FL production pathway, TCA cycle, and carboxylation reactions were compared under the different conditions. The targets are listed in Appendix B, Table A2.

In the proteome data, the C/N limited samples with 15% and 20% CO<sub>2</sub> enrichment grouped together while the 10% samples were closer to the control group (Figures 8–10).

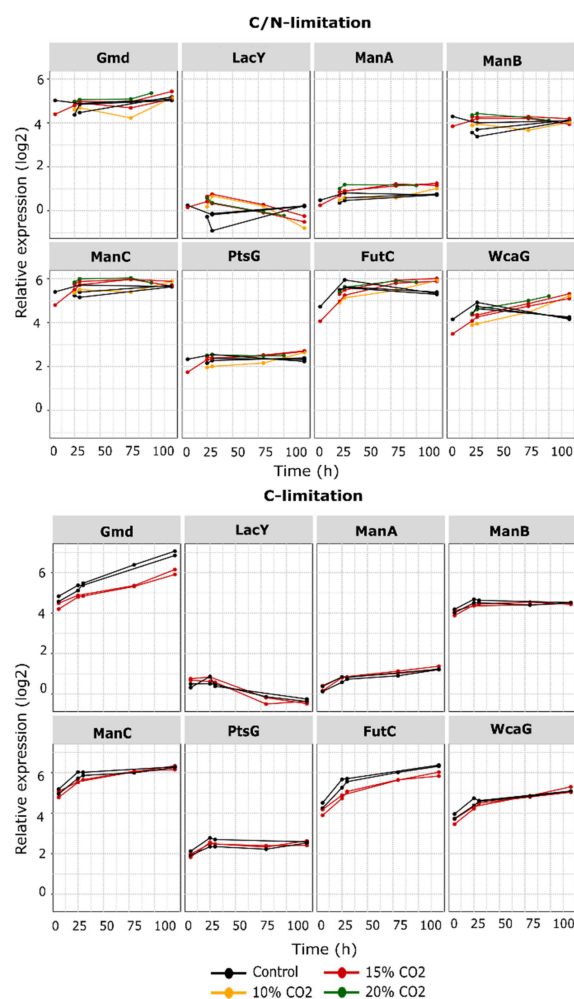


**Figure 8.** Expression profiles of proteins in the 2'-FL production pathway. Y-axis = relative expression in log<sub>2</sub>, X-axis = fermentation age after feed start (h). Gmd: GDP-mannose 4,6-dehydratase, LacY: lactose permease, ManA: mannose-6-phosphate isomerase, ManB: phosphomannomutase, ManC: mannose-1-phosphate guanyltransferase, PtsG: glucose-specific PTS enzyme IIBC component, FutC: alpha-1,2-fucosyltransferase, WcaG/Fcl: GDP-L-fucose synthase.

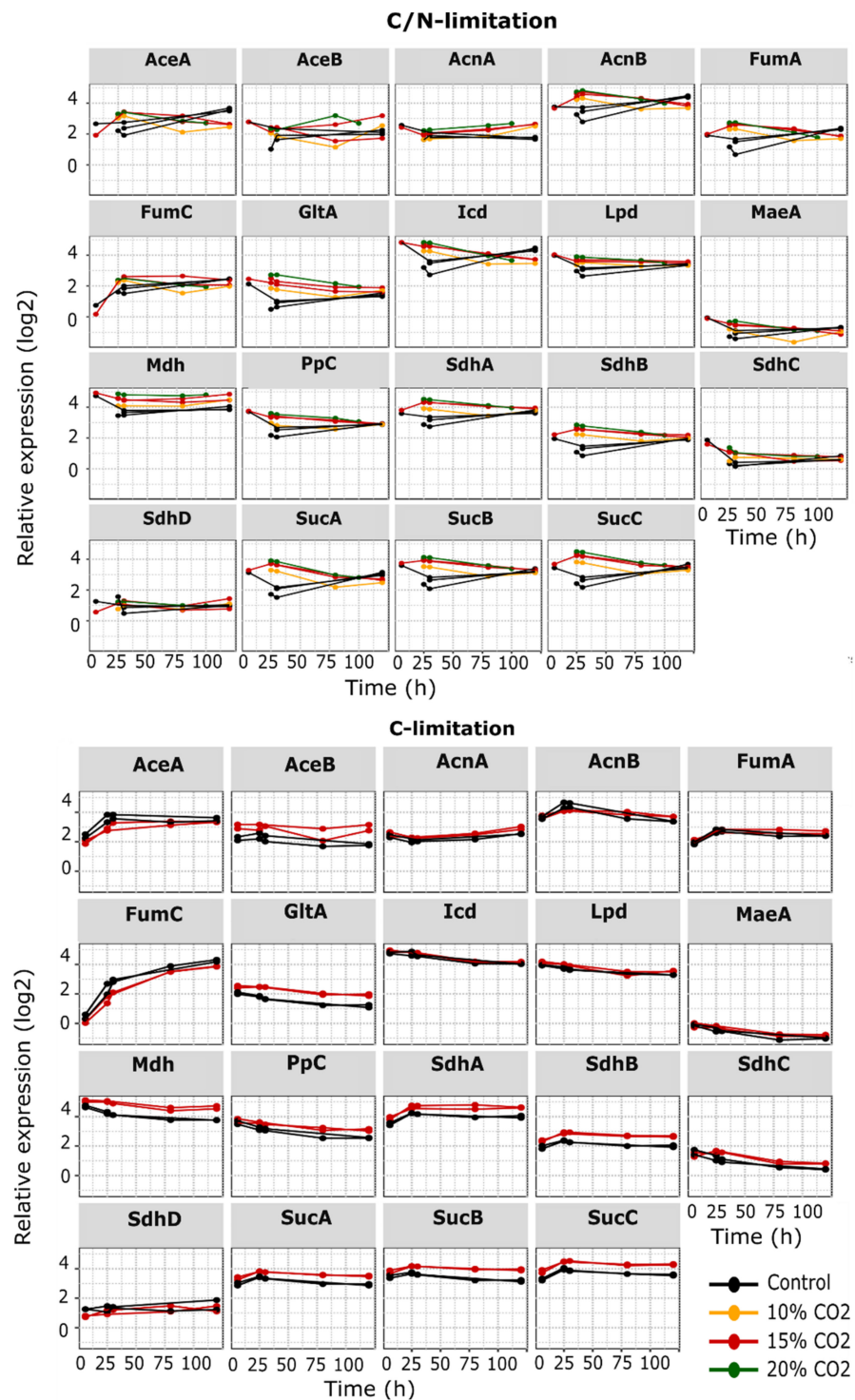


**Figure 9.** Protein expression level in the TCA cycle under different fermentation conditions: C/N- limited with 0%, 10%, 15%, and 20% pCO<sub>2</sub> enrichment and C-limited with 0% and 15% pCO<sub>2</sub> enrichment. Y-axis = relative expression in log<sub>2</sub>, X-axis = fermentation age after feed start in hours. AceB: malate synthase A, AceK: isocitrate dehydrogenase kinase, AcnA: aconitate hydratase A, AcnB: aconitate hydratase, FumA: fumarase A, FumC: Fumarate hydratase, GltA: citrate synthase, Icd: Isocitrate dehydrogenase, Lpd: lipoamide dehydrogenase, MaeA: malate dehydrogenase, Md: malate dehydrogenase, Ppc: Phosphoenolpyruvate carboxylase, SdhA: succinate:quinone oxidoreductase, SdhB: succinate:quinone oxidoreductase, SdhC: succinate:quinone oxidoreductase, SdhD: succinate:quinone oxidoreductase, SucA: 2-oxoglutarate decarboxylase, SucB: dihydrolipoyltranssuccinylase, SucD: succinyl-CoA synthetase subunit.

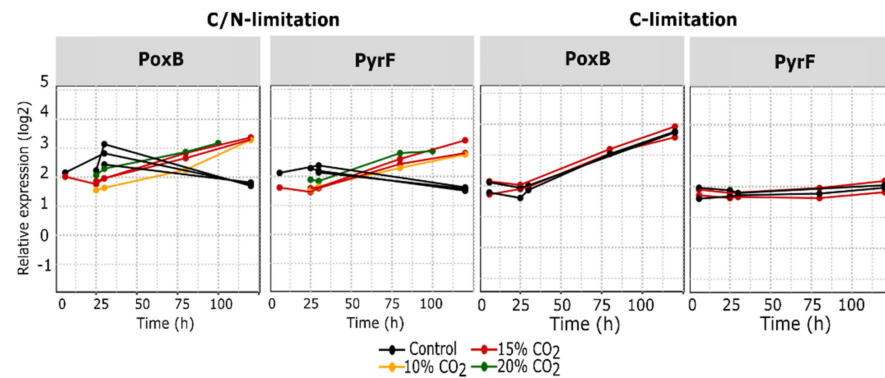


**Figure 10.** Changes in expression level of selected proteins involved in carboxylation and decarboxylation reactions. Y-axis = relative expression in  $\log_2$ , X-axis = fermentation age after feed start in hours. Ppc: Phosphoenolpyruvate carboxylase, PyrF: Orotidine 5'-phosphate decarboxylase, PoxB: Pyruvate oxidase.

### 3.5. Proteins from the 2'-FL Production Pathways Were Not Significantly Affected by $\text{CO}_2$ Enrichment

In general, the proteins directly involved with 2'-FL production were not drastically affected by the elevated  $\text{pCO}_2$  levels, regardless of the limitation state (Figure 8). In the C/N limited dataset, Fcl (WcaG), ManA, and FutC had a slightly higher abundance under  $\text{CO}_2$  enrichment at the late stage of the fermentation (Figure 8). Under C-limitation, a clear difference was observed in Gmd and FutC abundance, which both had lower expressions throughout the fermentation (Figure 8).

### 3.6. $\text{CO}_2$ Enrichment Increased TCA Cycle Protein Expression

In general, TCA related proteins were stably expressed under all tested conditions, but many of them were observed to be expressed at a higher level under  $\text{CO}_2$  enrichment (Figure 9). Although these patterns were highly reproducible, most of the fold changes did not reach the minimum threshold of  $|\text{FC}| = 1.5$  in the DEA. Therefore, in strict terms, none of the TCA target proteins had a significantly changed expression under the C-limited condition. On the other hand, several TCA enzymes such as GltA, SucAB, and SdhAB were affected in the C/N limited condition.

### 3.7. Enzymes Involved in Carboxylation and Decarboxylation Reactions

It was hypothesized that  $\text{pCO}_2$  levels could affect the expression of enzymes involved in carboxylation and decarboxylation reactions. Therefore, a total of 11 proteins involved in carboxylation (Ppc and Psd) and decarboxylation (MaeAB, PoxB, SucAB, Icd, AceF, PyrF, Lpd, NadC, and HemE) reactions were specifically examined in the dataset.

$\text{CO}_2$  enrichment under C-limited conditions led to higher SucAB expression throughout the fermentation process. However, this increase was also observed for the other proteins from the TCA cycle and is therefore not directly linked to changing decarboxylation kinetics (Figure 10). A similar pattern was observed under C/N limited conditions, but only until the middle part of the fermentation. At the late stage, the expression profiles of the  $\text{CO}_2$  enriched groups dropped and became similar to that of the control. On the other hand, PyrF, an orotidine-5'-phosphate decarboxylase catalyzing the last step in the pyrimidine synthesis, started low but had an increasingly higher expression after 30 h (Figure 10). This behavior was not observed in the C-limited dataset. The expression pattern of other decarboxylases such as Psd, HemE, and NadC were similar to PyrF in the C/N limited dataset but the differences between the conditions were not enhanced to the same extent (Appendix D, Figure A2). Surprisingly, except for Ppc, none of the targeted carboxylases were impacted by the  $\text{pCO}_2$  levels under solely C-limitation. For Ppc, the abundance was higher with  $\text{CO}_2$  enrichment under both C and C/N limited conditions (Figure 10).

### 3.8. Nitrogen Uptake Proteins

As expected, proteins involved in nitrogen assimilation were differentially expressed when comparing the C- and C/N-limited datasets. This was shown in the expression profiles of GlnA, GltB, and GltD (Appendix E, Figure A3). In the C/N limited condition, GlnA expression was increased at the timepoint when the culture reached ammonium limitation approximately 40 h into the fed-batch phase. It was also clear that the high expression of GlnA started later in the CO<sub>2</sub> enriched samples showing that CO<sub>2</sub> enrichment delayed the start of the nitrogen limitation.

## 4. Discussion

Based on the results from previous studies [18,19] and observed differences between large- and laboratory-scale fermentations, we expected to see increased pCO<sub>2</sub> levels effect product and biomass yields at a lower level of enrichment than what was actually observed. The absence of any clear impact at 10% enrichment was surprising considering the measured pCO<sub>2</sub> level in the large-scale fermentation was substantially lower than what this enrichment yielded throughout most of the fermentation (Figure 3). However, as the results reported by [18,19] were performed under very different physiological conditions with cultures grown in batch-mode and producing a protein instead of a metabolite, this could indicate that the impact of pCO<sub>2</sub> is different depending on growth rate, and perhaps imposed production demand, medium composition, and nutrient availability. The observed differences in biomass and product yields between factory and laboratory even after CO<sub>2</sub> enrichment thus provided a hint of other scale dependent factors being at work. It should be noted that we were not able to closely replicate the large-scale CO<sub>2</sub> profile in the scale-down reactor as we could only enrich with a fixed percentage in the inlet gas stream. The large-scale vessel would therefore always have a more dynamic CO<sub>2</sub> profile with larger differences between the peaks and troughs (Figure 3). Nonetheless, the pCO<sub>2</sub> level in the large-scale fermentation was within the range encompassed by the 0% and 10% enrichments but for a few hours at the very peak in the early fermentation phase (Figure 3). While the 10% enrichment did not show a significant impact, this could be achieved by increasing the CO<sub>2</sub> enrichment to 15% or 20%. While these enrichment levels resulted in a CO<sub>2</sub> level that was higher than what was observed in our process, they were still within a range that is encountered in industrial operations [19].

A further increase of the CO<sub>2</sub> enrichment up to 30% was also tested. This led to rapid acetic acid accumulation and a loss of culture viability shortly after the enrichment was initiated (Figure 6C,D). A likely explanation is that the high pCO<sub>2</sub> level impacted the growth rate of the strain. The feeding profile used in this study was designed to avoid an accumulation of acetate from overflow metabolism [32,33]. However, if the  $\mu_{max}$  was significantly reduced by the elevated pCO<sub>2</sub> levels, the threshold growth rate where acetate accumulation started was likely also reduced. Since the accumulation of acetate also reduces the  $\mu_{max}$  [32,34–36], this can quickly lead to a negative spiral with ever more acetate formation and growth rate reduction, eventually leading to a complete loss of the culture. This was precisely what was seen with very high base titration indicating that acid accumulation was already at the onset of the CO<sub>2</sub> enrichment which continued to increase until the cultivation collapsed (Appendix C, Figure A1). The formation of high levels of acids was confirmed by an end point measurement of 32.5 g/L (542 mM) acetic acid, a level that is toxic to *E. coli* and highly inhibitory to growth [36,37]. This behavior also closely mimicked what we have observed when we increased feed rates in the past. These results together with reported results in the literature show that the precise onset of pCO<sub>2</sub> growth inhibition is highly dependent on the organism and the growth conditions. Castan et al. reported a negative impact of 9.75% CO<sub>2</sub> enrichment with *E. coli* K12, that was further reduced to 19.48%, whereas Baez et al. reported a positive impact at 20 mbar, which turned negative at 70 mbar also using a K12 strain [19]. The negative impact was then magnified when increasing the pCO<sub>2</sub> level further to 150 mbar and 300 mbar. In contrast, Knoll et al. surprisingly did not report any negative impacts on growth even when CO<sub>2</sub> accumulated

to a level of 800 mbar in an aerobic glycerol-limited fed-batch process under highly elevated pressure [21]. This  $p\text{CO}_2$  level was much higher than the maximum level of 260 mbar that was measured in the 30% enriched fermentations that led to a rapid culture loss with our process. The growth rate resulting from the feeding profile they used was also significantly higher following a feeding profile corresponding to a  $\mu$  of  $0.153 \text{ h}^{-1}$ , which should make the situation even worse. However, it should be noted that we have observed that the heavy burden of metabolic pathway overexpression and metabolite production can reduce the threshold growth rate where overflow metabolism starts quite substantially and increase the sensitivity towards runaway acetic acid caused culture failures (data not shown). This has necessitated the use of less aggressive feeding profiles in our process. A key difference was also that they used a stepwise increase in pressure and thereby  $p\text{CO}_2$  level and that their fermentation was much shorter. Indeed, they did observe a dramatic increase in osmotic pressure after 22 h together with an accumulation of mixed acids indicating that the growth would not be sustainable for long at this pressure and  $p\text{CO}_2$  level.

Due to the particular traits of the process, this study also looked into the impact of sole carbon and C-N double limitation and how these limitations interacted with increased  $p\text{CO}_2$  levels. The potential for combining C-limitation with another nutrient limitation to redirect part of the carbon and energy consumption from the biomass into product formation is well known and can be an attractive choice for industrial production [38], [39]. Here, C/N-limited conditions were indeed shown to reduce biomass formation and increase product yield compared to C-limitation alone. In contrast to C/N-limitation, under C-limitation, no impact on biomass yield could be seen with the 15%  $p\text{CO}_2$  enrichment. This implied that the increased biomass in the 15%  $p\text{CO}_2$  enriched C/N-limited runs were indeed a result of increased nitrogen availability. The product yields for the C-, C/N- and, large-scale runs were also very close until approximately 30 h, which corresponded with the onset of N-limitation (Figure 6). After this point, the large-scale fermentation increased its carbon allocation to  $\text{CO}_2$  and decreased its allocation to the biomass and products. Thus, maintenance energy requirements were unanticipatedly increased. It is unknown whether this was caused by a change in physiology at the onset of C/N-limitation to one that was less well suited to the large-scale environment or if it coincided with a change in the mixing regime resulting in increased gradients in the large vessel as the volume increased and different impellers were engaged. In light of this result, it would be interesting to see if a relief of N-limitation could improve the yields post 30 h in large-scale fermentations.

The proteome analysis revealed that high  $p\text{CO}_2$  levels induced a greater number of differentially expressed proteins under C/N-limited conditions than C-limited. This was no surprise considering that the elevated  $\text{CO}_2$  level indirectly affected the degree of N-limitation by increasing the  $\text{NH}_4\text{OH}$  titration, which was expected to have a major impact on the physiology. We did observe an increased GadBCE and GlsA glutaminase expression under both C-limited and C/N-limited conditions. Though the differential expression did not show up after filtering in the C-limited samples and only after 120 h in the C/N-limited fermentations. This response suggested that the intracellular pH was acidified by dissolved  $\text{CO}_2$ . This has also been reported in other studies where  $\text{CO}_2$  triggered an acid response [40] or an increased GadABC expression level [18]. A general trend of higher expression values for TCA related proteins when exposed to  $\text{CO}_2$  enrichment was also observed for both C- and C/N-limited cultures. Since  $\text{CO}_2$  enrichment did not result in increased biomass formation under C-limitation, the higher TCA expression of especially GltA, Ppc, SdhAB, and SucABC was not likely a result of increased anaplerosis. However, it must be noted that reactions affected by high  $p\text{CO}_2$  levels would not necessarily lead to enzyme level changes.

A general trend of higher expression values for TCA related proteins when exposed to  $\text{CO}_2$  enrichment was also observed for both C- and C/N-limited cultures. This observation was the opposite of what Baez et al. found in their study, which showed lower carbon flux to TCA and reduced biomass yield under batch conditions. This was not unexpected as the growth rate in our fed-batch fermentations was much lower than the non-limited growth rate under batch conditions and was therefore not exhibiting overflow metabolism.

Interestingly, the C-limited samples showed a higher expression of most TCA enzymes even in the control condition at all timepoints. A higher expression of SucABC in the CO<sub>2</sub> enriched samples also suggested a higher flux in the TCA cycle and/or increased nitrogen assimilation. A higher TCA cycle flux could be related to increased Ppc (phosphoenolpyruvate carboxylase) activity, which has been observed to be upregulated in *Saccharomyces cerevisiae* under high CO<sub>2</sub> concentrations [41]. Ppc fixates CO<sub>2</sub> by carboxylation of the less reactive bicarbonate anion (HCO<sub>3</sub><sup>-</sup>) in the cytoplasm to form oxaloacetate from phosphoenolpyruvate [42]. In addition to being upregulated in our dataset, its reaction would be favored by higher pCO<sub>2</sub> levels and increase the supply of oxaloacetate to the TCA cycle.

Surprisingly, along with the upregulation of the L-malate dehydrogenase Mdh in the TCA cycle, a decarboxylating D-malate dehydrogenase DmlA was also upregulated, whereas MaeAB, a decarboxylating L-malate dehydrogenase, did not change its expression. The DmlA enzyme reduces D-malate to pyruvate and CO<sub>2</sub> under anaerobic conditions and it is also involved in L-leucine biosynthesis [43]. Lukas et al. found that DmlA was essential for growth on D-malate under aerobic conditions and other C4-dicarboxylates were also seen to induce *dmlA* such as L- and meso-tartrate, while succinate did not trigger the expression [43]. From the data we have, we could not find an explanation for why it was induced under the tested conditions.

## 5. Conclusions

This study was designed to test how elevated pCO<sub>2</sub> levels affect *E. coli* physiology and whether high pCO<sub>2</sub> concentration observed in a very large industrial fed-batch process could account for the reduced product yield compared to the same process at the laboratory-scale. While it was not possible to obtain a close mimic of the pCO<sub>2</sub> profile in the laboratory, it was observed that a process with 10% enrichment, which produced an equal or higher pCO<sub>2</sub> level (of around 110 mbar) compared to the 450 m<sup>3</sup> vessel throughout most of the process, did not affect the product formation. Therefore, other factors, alone or in combination with elevated pCO<sub>2</sub>, are required to account for the observed yield difference between the scales. The main candidate would be chemical gradients formed by the longer mixing times in the large vessel where particular variations in glucose concentration would be a prime suspect. However, increasing the pCO<sub>2</sub> concentration beyond the level that was seen with the 10% enrichment by using 15% enrichment did impact product and biomass yields and increasing it further to 30% caused a full collapse of the culture. While both C and C/N limited cultures saw reductions in product yield, the CO<sub>2</sub> enrichment only affected the biomass yield for the C/N-limited cultures indicating that this effect was due to a reduction of the degree of N-limitation. This was also reflected in the proteomics analysis which revealed surprisingly few changes for the C-limited condition. Here, the major differentially expressed proteins were in the TCA cycle, the two 2'-FL pathway related proteins Gmd and FutC, and the proteins involved in the acid stress response. Of these, changes to the TCA cycle and the 2'-FL pathway could potentially impact yields. However, the C-limited yield difference mainly manifested in the beginning of the fermentation when the proteomics differences in the 2'-FL pathway were very small. Thus, changes to the energetics, in which the TCA cycle plays a part, seems a more likely candidate.

**Author Contributions:** G.G. and T.J. designed the study and wrote the manuscript. G.G. acquired and analyzed the fermentation data. G.G. acquired and analyzed the proteomics data. A.V. performed proteomics analysis. G.G. performed visualization. P.B., M.K. and A.V. revised the manuscript for scientific content. All authors have read and agreed to the published version of the manuscript.

**Funding:** This research was partially funded by the Innovation Fund Denmark, grant number [8053-00209B].

**Institutional Review Board Statement:** Not applicable.

**Informed Consent Statement:** Not applicable.

**Data Availability Statement:** Restrictions apply to the availability of these data. The limited dataset that supports the findings of this study are available upon reasonable request from the authors and with the permission of Royal DSM.

**Acknowledgments:** We thank our colleagues at DSM Hørsholm and Delft helping with analytical support and fruitful discussions.

**Conflicts of Interest:** The authors declare no conflict of interest.

## Appendix A

**Table A1.** Overview of the fermentations in the study. The number of replicate fermentations carried out for each condition is summarized as well as the number of fermentations used for the proteomics study. Sample timepoints for the proteomics study are listed.

CO <sub>2</sub> Enrichment	Nutrient Limitation	Number of Replicate Fermentations	Number of Fermentations Sampled for Proteomics	Timepoints for Proteomics Sampling
Control (0%)	C/N	4	3	6 h
				30 h
				120 h
Control (0%)	C	3	2	6 h
				30 h
				80 h
15% enriched	C	2	2	120 h
				6 h
				30 h
10% enriched	C/N	1	1	80 h
				30 h
				120 h
15% enriched	C/N	3	2	6 h
				30 h
				80 h
20% enriched	C/N	2	1	120 h
				6 h
				30 h
30% enriched	C/N	2	n/a	80 h
				100 h
				n/a

## Appendix B

**Table A2.** The list of proteins included in the targeted search in the proteomics dataset. The list is divided into three functional groups: TCA cycle and pyruvate metabolism, 2FL production pathway, and Decarboxylation/carboxylation related proteins.

TCA Cycle/Pyruvate Metabolism		2'-FL Production	
Protein	Function	Protein	Function
AceB	malate synthase A	Gmd	GDP-mannose 4,6-dehydratase
AceK	isocitrate dehydrogenase kinase/isocitrate dehydrogenase phosphatase	LacY	lactose permease
AcnA	aconitate hydratase A	ManA	mannose-6-phosphate isomerase
AcnB	bifunctional aconitate hydratase B and 2-methylisocitrate dehydratase	ManB	phosphomannomutase
FumA	fumarase A	ManC	mannose-1-phosphate guanylyltransferase
FumC	Fumarate hydratase	PtsG	glucose-specific PTS enzyme IIBC component

Table A2. Cont.

TCA Cycle/Pyruvate Metabolism		2'-FL Production	
GltA	citrate synthase	FutC	fucosyltransferase
Icd	Isocitrate dehydrogenase	WcaG/Fcl	GDP-L-fucose synthase
Lpd	lipoamide dehydrogenase	Decarboxylation/Carboxylation	
MaeA	NAD <sup>+</sup> -dependent malate dehydrogenase	Protein	Function
Mdh	malate dehydrogenase	Ppc	Phosphoenolpyruvate carboxylase
Ppc	Phosphoenolpyruvate carboxylase	AceF	Acetyltransferase, component of pyruvate dehydrogenase complex
SdhA	succinate:quinone oxidoreductase, FAD binding protein	PyrF	Orotidine 5'-phosphate decarboxylase
SdhB	succinate:quinone oxidoreductase, iron-sulfur cluster binding protein	NadC	Nicotinate-nucleotide pyrophosphorylase, decarboxylating
SdhC	succinate:quinone oxidoreductase, membrane protein	HemE	Uroporphyrinogen decarboxylase
SdhD	succinate:quinone oxidoreductase, membrane protein	Psd	Phosphatidylserine decarboxylase proenzyme
SucA	2-oxoglutarate decarboxylase, thiamine-requiring	SucB	succinyltransferase component of 2-oxoglutarate dehydrogenase
SucB	dihydrolipoyltranssuccinylase	SucA	2-oxoglutarate decarboxylase
SucD	succinyl-CoA synthetase subunit α	LpdA	lipoamide dehydrogenase
		Icd	isocitrate dehydrogenase
		PoxB	Pyruvate oxidase
		MaeA	malate dehydrogenase, oxaloacetate-decarboxylating and NAD <sup>+</sup> dependent
		MaeB	malate dehydrogenase, oxaloacetate-decarboxylating and NADP <sup>+</sup> dependent

Appendix C

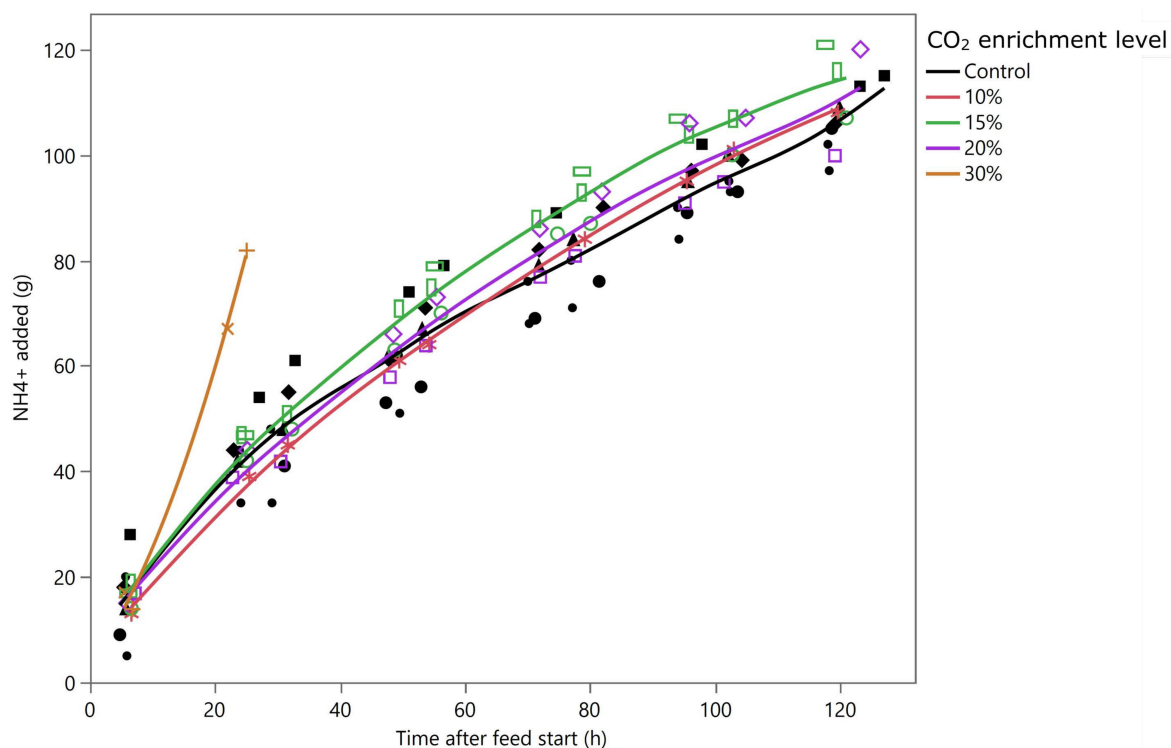
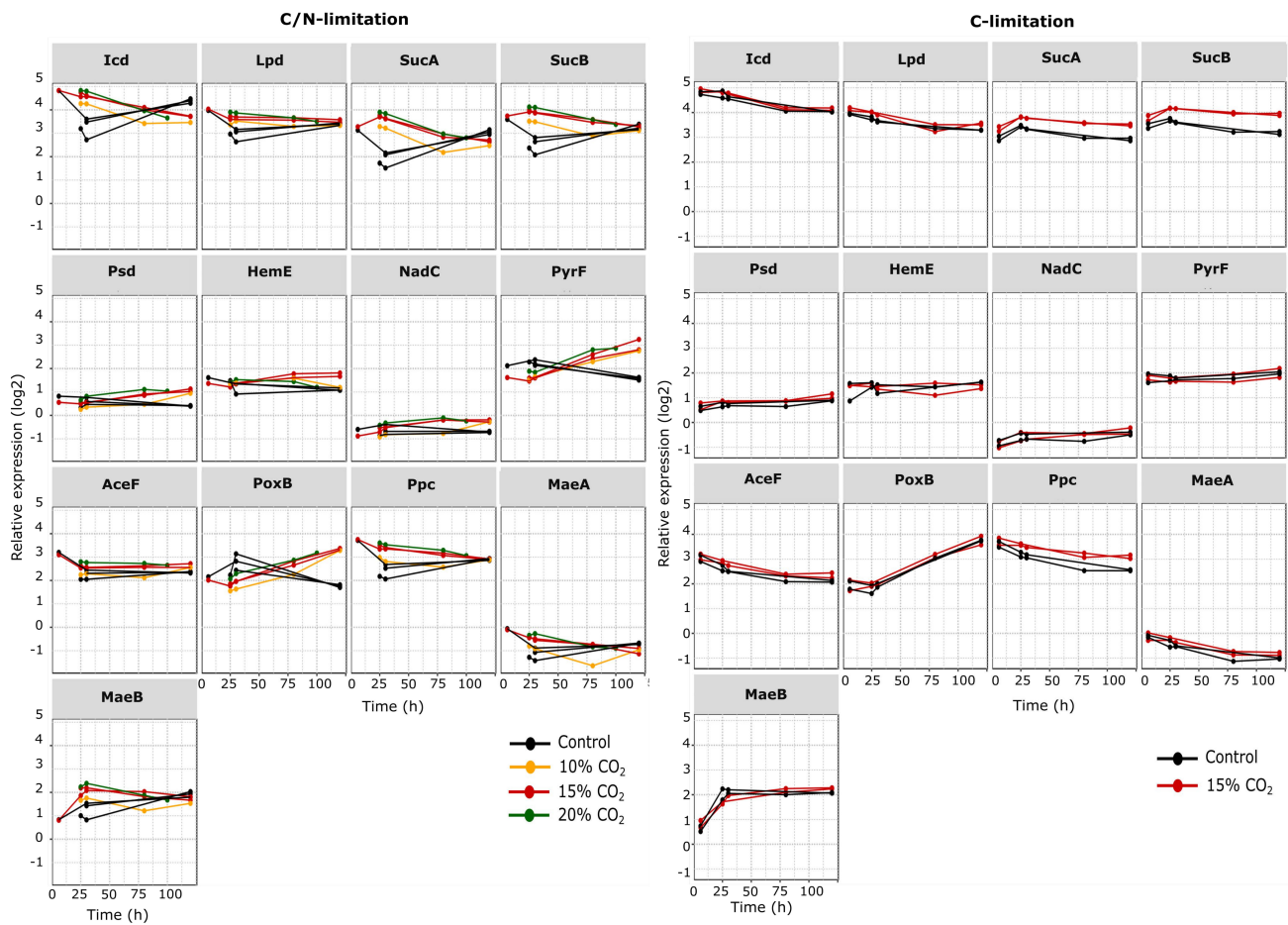


Figure A1. Ammonium (NH<sub>4</sub><sup>+</sup>) addition for C/N condition with different CO<sub>2</sub> enrichment levels for experiments with C/N limitation. The gravimetric NH<sub>4</sub><sup>+</sup> addition was calculated from the base addition consisting of NH<sub>4</sub>OH. Each symbol represents a distinct experiment.

Appendix D



**Figure A2.** Changes in expression level of selected proteins involved in carboxylation and decarboxylation reactions. Y-axis = relative expression in log<sub>2</sub>, X-axis = fermentation age after feed start in hours. Ppc: Phosphoenolpyruvate carboxylase, AceF: Acetyltransferase, PyrF: Orotidine 5'-phosphate decarboxylase, NadC: Nicotinate-nucleotide pyrophosphorylase, decarboxylating, HemE: Uroporphyrinogen decarboxylase, Psd: Phosphatidylserine decarboxylase proenzyme, SucA: 2-oxoglutarate decarboxylase, SucB: succinyltransferase, LpdA: lipoamide dehydrogenase, Icd: isocitrate dehydrogenase, PoxB: Pyruvate oxidase, MaeA: malate dehydrogenase, oxaloacetate-decarboxylating, MaeB: malate dehydrogenase, oxaloacetate-decarboxylating.

## Appendix E

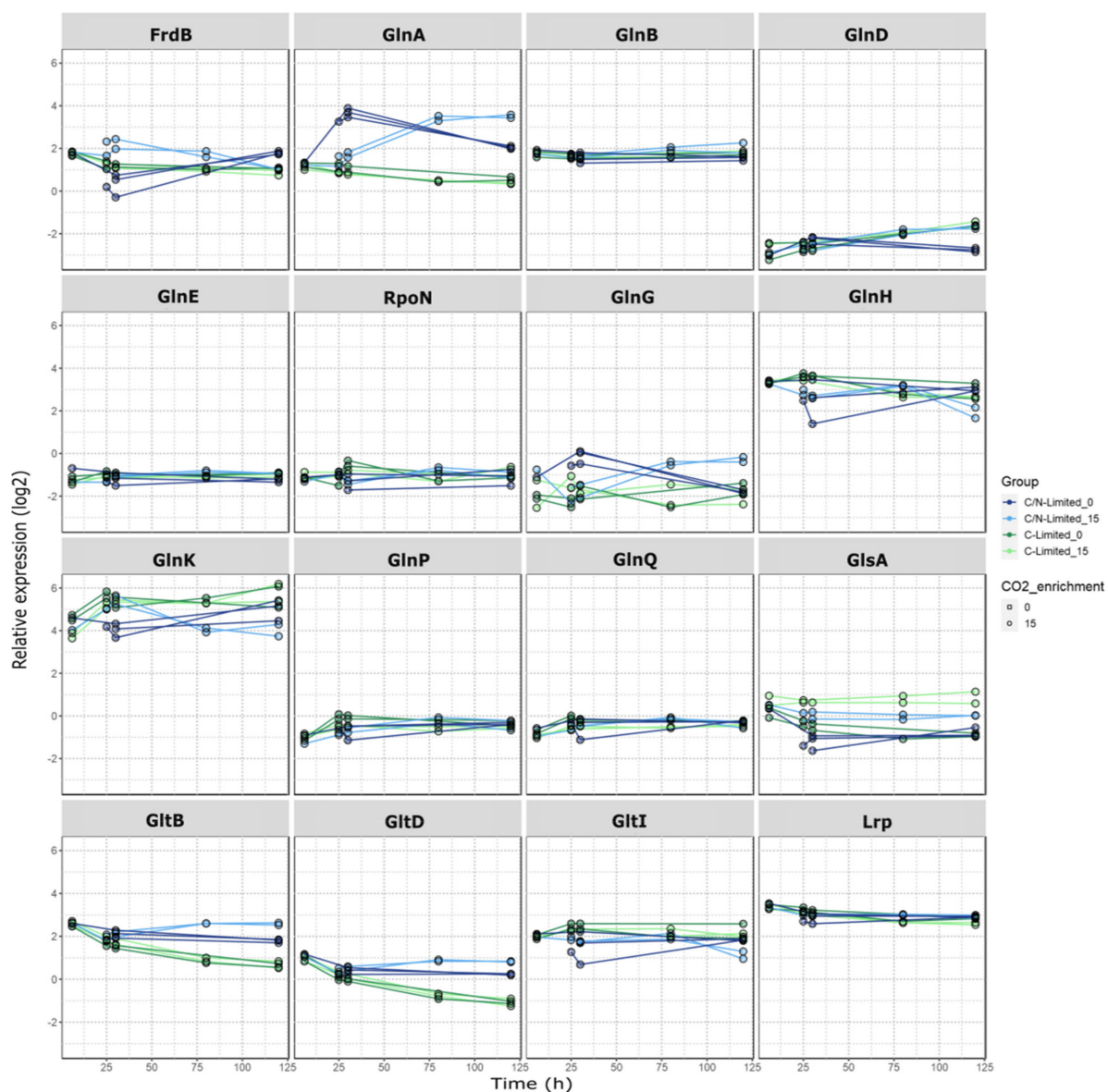


**Figure A3.** Expression profile of acid stress and nitrogen assimilation related proteins. Y-axis: relative expression in log<sub>2</sub> of proteins involved in acid stress response and nitrogen assimilation. X-axis: fermentation time after feed start.

## References

1. Sakanaka, M.; Hansen, M.E.; Gotoh, A.; Katoh, T.; Yoshida, K.; Odamaki, T.; Yachi, H.; Sugiyama, Y.; Kurihara, S.; Hirose, J.; et al. Evolutionary adaptation in fucosyllactose uptake systems supports bifidobacteria-infant symbiosis. *Sci. Adv.* **2019**, *5*, eaaw7696. [[CrossRef](#)]
2. Brand-Müller, J.C.; McVeagh, P.; McNeil, Y.; Messer, M. Digestion of human milk oligosaccharides by healthy infants evaluated by the lactulose hydrogen breath test. *J. Pediatr.* **1998**, *133*, 95–98. [[CrossRef](#)]
3. Hester, S.N.; Husted, D.S.; Mackey, A.D.; Singhal, A.; Marriage, B.J. Is the Macronutrient Intake of Formula-Fed Infants Greater Than Breast-Fed Infants in Early Infancy? *J. Nutr. Metab.* **2012**, *2012*, 1–13. [[CrossRef](#)] [[PubMed](#)]
4. Soyylmaz, B.; Mikš, M.H.; Röhrig, C.H.; Matwiejuk, M.; Meszaros-Matwiejuk, A.; Vignæs, L.K. The Mean of Milk: A Review of Human Milk Oligosaccharide Concentrations throughout Lactation. *Nutrients* **2021**, *13*, 2737. [[CrossRef](#)]
5. Ammann, R. Achieving the impossible: Jennewein Biotechnology is dedicated to the production of human milk oligosaccharides. *Eur. Dairy Mag.* **2017**, *5*, 30–31.

6. Bych, K.; Mikš, M.H.; Johanson, T.; Hederos, M.J.; Vignsnaes, L.K.; Becker, P. Production of HMOs using microbial hosts—From cell engineering to large scale production. *Curr. Opin. Biotechnol.* **2018**, *56*, 130–137. [[CrossRef](#)]
7. Larsson, G.; Törnkvist, E.; Ståhl Wernersson, C.; Trägårdh, H.; Noorman, H.; Enfors, S.-O. Substrate gradients in bioreactors: Origin and consequences. *Bioprocess Biosyst. Eng.* **1996**, *14*, 281–289. [[CrossRef](#)]
8. Sandoval-Basurto, E.A.; Gosset, G.; Bolívar, F.; Ramírez, O.T. Culture of *Escherichia coli* under dissolved oxygen gradients simulated in a two-compartment scale-down system: Metabolic response and production of recombinant protein. *Biotechnol. Bioeng.* **2004**, *89*, 453–463. [[CrossRef](#)]
9. Lara, A.R.; Leal, L.; Flores, N.; Gosset, G.; Bolívar, F.; Ramírez, O.T. Transcriptional and metabolic response of recombinant *Escherichia coli* to spatial dissolved oxygen tension gradients simulated in a scale-down system. *Biotechnol. Bioeng.* **2005**, *93*, 372–385. [[CrossRef](#)]
10. Cortés, J.T.; Flores, N.; Bolívar, F.; Lara, A.R.; Ramírez, O.T. Physiological effects of pH gradients on *Escherichia coli* during plasmid DNA production. *Biotechnol. Bioeng.* **2015**, *113*, 598–611. [[CrossRef](#)]
11. Crater, J.S.; Lievens, J.C. Scale-up of industrial microbial processes. *FEMS Microbiol. Lett.* **2018**, *365*, fny138. [[CrossRef](#)]
12. Junker, B.H. Scale-up methodologies for *Escherichia coli* and yeast fermentation processes. *J. Biosci. Bioeng.* **2004**, *97*, 347–364. [[CrossRef](#)]
13. McIntyre, M.; McNeil, B. Effects of elevated dissolved CO<sub>2</sub> levels on batch and continuous cultures of *Aspergillus niger* A60: An evaluation of experimental methods. *Appl. Environ. Microbiol.* **1997**, *63*, 4171–4177. [[CrossRef](#)]
14. Zhu, M.M.; Goyal, A.; Rank, D.L.; Gupta, S.K.; Boom, T.V.; Lee, S.S. Effects of Elevated pCO<sub>2</sub> and Osmolality on Growth of CHO Cells and Production of Antibody-Fusion Protein B1: A Case Study. *Biotechnol. Prog.* **2008**, *21*, 70–77. [[CrossRef](#)]
15. Sander, R. Compilation of Henry's law constants (version 4.0) for water as solvent. *Atmospheric Chem. Phys.* **2015**, *15*, 4399–4981. [[CrossRef](#)]
16. Lara, A.R.; Taymaz-Nikerel, H.; Mashego, M.R.; van Gulik, W.M.; Heijnen, J.J.; Ramírez, O.T.; van Winden, W.A. Fast dynamic response of the fermentative metabolism of *Escherichia coli* to aerobic and anaerobic glucose pulses. *Biotechnol. Bioeng.* **2009**, *104*, 1153–1161. [[CrossRef](#)]
17. Simen, J.D.; Löffler, M.; Jäger, G.; Schäferhoff, K.; Freund, A.; Matthes, J.; Müller, J.; Takors, R.; Team, R.N. Transcriptional response of *Escherichia coli* to ammonia and glucose fluctuations. *Microb. Biotechnol.* **2017**, *10*, 858–872. [[CrossRef](#)]
18. Baez, A.; Flores, N.; Bolívar, F.; Ramírez, O.T. Simulation of dissolved CO<sub>2</sub> gradients in a scale-down system: A metabolic and transcriptional study of recombinant *Escherichia coli*. *Biotechnol. J.* **2011**, *6*, 959–967. [[CrossRef](#)]
19. Baez, A.; Flores, N.; Bolívar, F.; Ramírez, O.T. Metabolic and transcriptional response of recombinant *Escherichia coli* to elevated dissolved carbon dioxide concentrations. *Biotechnol. Bioeng.* **2009**, *104*, 102–110. [[CrossRef](#)]
20. Castan, A.; Näsman, A.; Enfors, S.-O. Oxygen enriched air supply in *Escherichia coli* processes: Production of biomass and recombinant human growth hormone. *Enzym. Microb. Technol.* **2002**, *30*, 847–854. [[CrossRef](#)]
21. Knoll, A.; Bartsch, S.; Husemann, B.; Engel, P.; Schroer, K.; Ribeiro, B.; Stöckmann, C.; Seletzky, J.; Büchs, J. High cell density cultivation of recombinant yeasts and bacteria under non-pressurized and pressurized conditions in stirred tank bioreactors. *J. Biotechnol.* **2007**, *132*, 167–179. [[CrossRef](#)] [[PubMed](#)]
22. Liao, H.; Zhang, F.; Hu, X.; Liao, X. Effects of high-pressure carbon dioxide on proteins and DNA in *Escherichia coli*. *Microbiology* **2011**, *157*, 709–720. [[CrossRef](#)]
23. Ballestra, P.; DA Silva, A.A.; Cuq, J. Inactivation of *Escherichia coli* by Carbon Dioxide under Pressure. *J. Food Sci.* **1996**, *61*, 829–831. [[CrossRef](#)]
24. Oulé, M.K.; Tano, K.; Bernier, A.-M.; Arul, J. *Escherichia coli* inactivation mechanism by pressurized CO<sub>2</sub>. *Can. J. Microbiol.* **2006**, *52*, 1208–1217. [[CrossRef](#)] [[PubMed](#)]
25. Eklund, T. The effect of carbon dioxide on bacterial growth and on uptake processes in bacterial membrane vesicles. *Int. J. Food Microbiol.* **1984**, *1*, 179–185. [[CrossRef](#)]
26. Zanghi, J.A.; Schmelzer, A.E.; Mendoza, T.P.; Knop, R.H.; Miller, W.M. Bicarbonate concentration and osmolality are key determinants in the inhibition of CHO cell polysialylation under elevated pCO<sub>2</sub> or pH. *Biotechnol. Bioeng.* **1999**, *65*, 182–191. [[CrossRef](#)]
27. Dixon, N.M.; Kell, D.B. The inhibition by CO<sub>2</sub> of the growth and metabolism of micro-organisms. *J. Appl. Bacteriol.* **1989**, *67*, 109–136. [[CrossRef](#)]
28. Amoabediny, G.; Büchs, J. Determination of CO<sub>2</sub> sensitivity of micro-organisms in shaken bioreactors. I. Novel method based on the resistance of sterile closure. *Biotechnol. Appl. Biochem.* **2010**, *57*, 157–166. [[CrossRef](#)]
29. Pedersen, M.; Papadakis, M. Nucleic Acid Construct for In Vitro and In Vivo Gene Expression. Denamrk Patent WO2019123324A1, 27 June 2019.
30. Bruderer, R.; Bernhardt, O.M.; Gandhi, T.; Miladinović, S.M.; Cheng, L.-Y.; Messner, S.; Ehrenberger, T.; Zanotelli, V.R.T.; Butscheid, Y.; Escher, C.; et al. Extending the Limits of Quantitative Proteome Profiling with Data-Independent Acquisition and Application to Acetaminophen-Treated Three-Dimensional Liver Microtissues. *Mol. Cell. Proteom.* **2015**, *14*, 1400–1410. [[CrossRef](#)]
31. Löffler, M.; Simen, J.D.; Müller, J.; Jäger, G.; Laghrami, S.; Schäferhoff, K.; Freund, A.; Takors, R. Switching between nitrogen and glucose limitation: Unraveling transcriptional dynamics in *Escherichia coli*. *J. Biotechnol.* **2017**, *258*, 2–12. [[CrossRef](#)]
32. Bernal, V.; Cerezo, S.C.; Cánovas, M. Acetate metabolism regulation in *Escherichia coli*: Carbon overflow, pathogenicity, and beyond. *Appl. Microbiol. Biotechnol.* **2016**, *100*, 8985–9001. [[CrossRef](#)] [[PubMed](#)]

33. Xu, B.; Jahic, M.; Enfors, S.-O. Modeling of Overflow Metabolism in Batch and Fed-Batch Cultures of *Escherichia coli*. *Biotechnol. Prog.* **1999**, *15*, 81–90. [[CrossRef](#)] [[PubMed](#)]
34. Turner, C.; Gregory, M.E.; Turner, M.K. A study of the effect of specific growth rate and acetate on recombinant protein production of *Escherichia coli* JM107. *Biotechnol. Lett.* **1994**, *16*, 891–896. [[CrossRef](#)]
35. Luli, G.W.; Strohl, W.R. Comparison of growth, acetate production, and acetate inhibition of *Escherichia coli* strains in batch and fed-batch fermentations. *Appl. Environ. Microbiol.* **1990**, *56*, 1004–1011. [[CrossRef](#)] [[PubMed](#)]
36. Pinhal, S.; Ropers, D.; Geiselmann, J.; de Jong, H. Acetate Metabolism and the Inhibition of Bacterial Growth by Acetate. *J. Bacteriol.* **2019**, *201*, e00147-19. [[CrossRef](#)]
37. Trček, J.; Mira, N.P.; Jarboe, L.R. Adaptation and tolerance of bacteria against acetic acid. *Appl. Microbiol. Biotechnol.* **2015**, *99*, 6215–6229. [[CrossRef](#)] [[PubMed](#)]
38. Chubukov, V.; Desmarais, J.J.; Wang, G.; Chan, L.J.G.; Baidoo, E.E.K.; Petzold, C.J.; Keasling, J.D.; Mukhopadhyay, A. Engineering glucose metabolism of *Escherichia coli* under nitrogen starvation. *NPJ Syst. Biol. Appl.* **2017**, *3*, 16035. [[CrossRef](#)]
39. Morita, T.; Fukuoka, T.; Imura, T.; Kitamoto, D. Accumulation of cellobiose lipids under nitrogen-limiting conditions by two ustilaginomycetous yeasts, *Pseudozyma aphidis* and *Pseudozyma hubeiensis*. *FEMS Yeast Res.* **2013**, *13*, 44–49. [[CrossRef](#)]
40. Sun, L.; Fukamachi, T.; Saito, H.; Kobayashi, H. Carbon dioxide increases acid resistance in *Escherichia coli*. *Letts. Appl. Microbiol.* **2005**, *40*, 397–400. [[CrossRef](#)]
41. Aguilera, J.; Petit, T.; De Winde, J.H.; Pronk, J.T. Physiological and genome-wide transcriptional responses of *Saccharomyces cerevisiae* to high carbon dioxide concentrations. *FEMS Yeast Res.* **2005**, *5*, 579–593. [[CrossRef](#)]
42. Kai, Y.; Matsumura, H.; Izui, K. Phosphoenolpyruvate carboxylase: Three-dimensional structure and molecular mechanisms. *Arch. Biochem. Biophys.* **2003**, *414*, 170–179. [[CrossRef](#)]
43. Lukas, H.; Reimann, J.; Bin Kim, O.; Grimpo, J.; Uden, G. Regulation of Aerobic and Anaerobic d -Malate Metabolism of *Escherichia coli* by the LysR-Type Regulator DmlR (YeaT). *J. Bacteriol.* **2010**, *192*, 2503–2511. [[CrossRef](#)]